

Theoretical investigation of the non-degenerate four-wave mixing response for cyanine systems within the VB-CT model: Relation time's effects

J.L. Paz^{1} and E. Squitieri²*

¹*Departamento de Química, Universidad Simón Bolívar, Apartado 89000.
Caracas 1080-A, Venezuela.*

²*Escuela de Química, Facultad de Ciencias, Universidad Central de Venezuela,
Apartado 47102. Caracas 1020-A, Venezuela.*

Recibido: 02-02-05 Aceptado: 14-09-05

Abstract

In this paper we present the calculations of the non-degenerate four wave-mixing (nd-FWM) signal for cyanine molecules in the context of the valence bond-charge transfer (VB-CT) model. In particular, we study the effect of alter the relation between the longitudinal (T_1) and transversal (T_2) relaxation times on this signal. As result of our calculations, only four peaks are observed in the nd-FWM spectrum in the frequency space, in contrast to twelve peaks observed for common push-pull chromophores. Moreover, significant changes in intensity and shape of the peaks of the nd-FWM spectrum with relation to the variation in the ratio between T_1 and T_2 were observed.

Key works: Cyanine; four-wave mixing (FWM); push-pull molecules; VB-CT model.

Investigación teórica de la respuesta de mezcla de cuatro ondas no-degenerada para sistemas de cianinas dentro del modelo VB-CT: Efectos de los tiempos de relajación

Resumen

En este artículo, presentamos el cálculo para la señal de la señal de mezcla de cuatro ondas no degenerada para moléculas de cianina, en el contexto del modelo VB-CT de enlace valencia-Transferencia de carga. En particular, estudiamos el efecto de alterar la relación entre los tiempos de relajación longitudinal (T_1) y transversal (T_2), sobre esta señal. Como resultados de nuestros cálculos, sólo 4 picos son observados en el espectro de la nd-FWM en el espacio de frecuencia, en contraste a 12 picos observados comúnmente para cromóforos push-pull. Sin embargo, cambios significativos fueron observados en intensidad y ancho de los picos del espectro de nd-FWM con relación a la variación en el cociente entre los tiempos de relajación.

Palabras clave: Cianinas; mezcla de cuatro ondas; moléculas puh-pull; modelo VB-CT.

* Premio Polar 2005, mención Química. To whom correspondence should be addressed. Phone: 58(212)9063954. E-mail: jlpaz@usb.ve.

1. Introduction

Non-linear optical (NLO) properties of organic molecules have been extensively studied because of their potential applications in electronic and optical devices (1, 2). Most studies for obtaining large NLO responses have focused on push-pull molecules in which the electron donor (D) and electron acceptor (A) groups are connected through a π -conjugation path (Figure 1). A general structure-property relationship for these D-A systems has been well understood although some further modifications and improvements are still ongoing (3, 4). It has been shown theoretically and experimentally that an enhanced NLO response can be achieved by optimizing the strength of the donor-acceptor pair and/or the nature of the conjugation path (5-8). Moreover, Marder and co-workers (9) studied the correlation between static (hyper)polarizabilities and ground-state geometries in terms of the bond length alternation (BLA) parameter, defined as the difference between the average length of adjacent carbon-carbon bonds in a polymethine chain. The main result obtained from this work was that the (hyper)polarizabilities of the D-A chromophores are sensitive to the molecular ground-state structures.

Cyanine molecules encompass a large variety of push-pull molecules. Among these the simplest cyanines are of the form: $\text{NH}_2-(\text{CH})_n-\text{NH}_2^+$ with n odd. It has been shown that theoretical calculations on these systems can play an important role in understanding the origin of their NLO properties and the establishment of the structure-property relationship for the electronic and

vibrational contribution to the molecular (hyper)polarizabilities (10). In this work, our main goal is to provide a direct correspondence between the ratio T_1/T_2 and intensity of the nd-FWM signal for $\text{NH}_2-(\text{CH})_3-\text{NH}_2^+$ cyanine. The analysis will be carried out with the help of VB-CT model, which has been used to describe the electronic-vibrational structure of push-pull polyenes (11), and Optical Bloch Equations (OBE) (12).

2. The VB-CT model for dipolar push-pull molecules

The VB-CT model (11) assumes that the electronic ground and excited state wave function (Ψ_{gr} and Ψ_{ex} , respectively) of the D-A molecule can be described using the linear combination of two orthogonal wave functions representing two resonant structures:

$$\Psi_{gr} = (1-f)^{1/2}\Psi_{VB} + f^{1/2}\Psi_{CT}, \quad [1]$$

and

$$\Psi_{ex} = f^{1/2}\Psi_{VB} - (1-f)^{1/2}\Psi_{CT}. \quad [2]$$

In Equations [1] and [2], the base function Ψ_{VB} corresponds to a neutral (VB) structure (no charge transfer from donor to acceptor) and to a charge-transfer (CT) structure. In the CT structure, one electron is completely transferred from the donor to the acceptor group while readjusting the other bonds, as illustrate in Figure 1. The fraction f of the CT configuration in the ground state is determined by the relative energy of Ψ_{VB} and Ψ_{CT} on Ψ_{gr} , the coupling

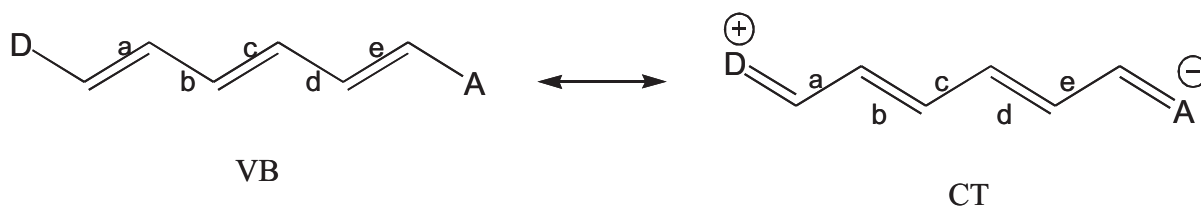


Figure 1. Valence-bond (VB) and charge-transfer (CT) configurations.

between them, the change in dipole moments and the solvent polarity.

Given a certain dipolar push-pull molecule, i.e., chosen D, A, and conjugated bridge, its structure in the electronic ground state will turn out to be intermediate between those in the VB and CT states and be determinate with the following reasoning.

In the harmonic approximation for the energy of the states VB and CT, the Hamiltonian matrix describing a linear push-pull polyene with a relevant vibrational mode, denoted by q , is:

$$H = \begin{pmatrix} (1/2)k(q - q_{VB}^0)^2 & -t \\ -t & V_0 + (1/2)k(q - q_{CT}^0)^2 \end{pmatrix} \quad [3]$$

where t represents the charge transfer integral (t is positive), V_0 corresponds to the electronic energy gap between the CT and VB states evaluated at its corresponding equilibrium positions q_{CT}^0 and q_{VB}^0 (with $q_{VB}^0 = -q_{CT}^0$) and k represents the force constant appropriate for the polyene linkers.

From Equations [1] and [3], the potential energy surface of the ground (-) and excited state (+) are given by:

$$U_{\pm}(q) = \frac{1}{2} \left\{ V_0 + \frac{k}{2} [(q - q_{VB}^0)^2 + (q - q_{CT}^0)^2] \pm \sqrt{(V_0 + k\delta q)^2 + 4t^2} \right\}, \quad [4]$$

where $\delta q = q_{VB}^0 - q_{CT}^0$ and q is identical to that BLA coordinate (11), which is located along the π -chain axis.

Since Ψ_{VB} and Ψ_{CT} involve alternate resonant descriptions of the intervening polyene unit, the increase of f from 0 to 1 will change each double bond (1.33 Å) of the polyene to a single bond (1.45 Å) and vice versa. Consequently, the BLA coordinate changes

from $q_{VB}^0 = -0.12 \text{ \AA}$ to $q_{CT}^0 = -0.12 \text{ \AA}$ as the CT fraction f goes from 0 to 1.

Using [4] the equilibrium BLA coordinate, $q_{eq.}$, is given by:

$$q_{eq.} = q_{VB}^0 - \delta f(q_{eq.}), \quad [5]$$

with $f(q_{eq.})$ as the squared coefficient corresponding to the Ψ_{CT} function in Ψ_{gr} evaluated at $q_{eq.}$:

$$f(q_{eq.}) = \frac{1}{2} \left\{ 1 - \frac{(V_0 + k\delta q_{eq.})}{\sqrt{(V_0 + k\delta q_{eq.})^2 + 4t^2}} \right\}. \quad [6]$$

To electronic ground state, large and positive V_0 values correspond to $q_{eq.}$ close to the VB (polyenic) structure (i.e. $f \rightarrow 0$), while large and negative V_0 values correspond to $q_{eq.}$ close to the CT (zwitterionic) structure (i.e. $f \rightarrow 1$). The case $V_0 = 0$ (i.e. $f \rightarrow 0.5$) corresponds to cyanine molecules.

Assuming that only the CT state has a large dipole moment as compared to that found in the VB state, i.e. $\mu_{CT} > \mu_{VB}$, the permanent dipole moment of the ground and excited state are, respectively, given by:

$$m_{gr}(q_{eq.}) = \langle \Psi_{VB} | \hat{m} | \Psi_{VB} \rangle = \mu_{CT} f(q_{eq.}), \quad [7]$$

and

$$m_{gr}(q_{eq.}) = \langle \Psi_{CT} | \hat{m} | \Psi_{CT} \rangle = \mu_{CT} [1 - f(q_{eq.})], \quad [8]$$

where $\mu_{CT} = Q|e|R_{DA}$ (11). In μ_{CT} expression, Q is the net fraction charge transfer for Ψ_{CT} resonance structure, and R_{DA} is the distance between donor-acceptor. The transition dipole moment between Ψ_{gr} and Ψ_{ex} states is:

$$m_{gr,ex}(q_{eq.}) = \langle \Psi_{VB} | \hat{m} | \Psi_{CT} \rangle = \mu_{CT} [1 - f(q_{eq.})]^{1/2} f^{1/2}(q_{eq.}). \quad [9]$$

3. The nd-FWM signal

In nd-FWM spectroscopy (13, 14) is employed a high-intensity laser beam (pump beam) with frequency ω_1 and a propagation vector \vec{k}_1 and another less intense laser beam (probe beam) with frequency ω_2 (with $\omega_1 \neq \omega_2$) and propagation vector \vec{k}_2 . Both laser beams are incident on a molecular medium with a small incidence angle θ between them ($\theta \sim 3^\circ$). The interactions among these fields generate a dispersion of signals of different frequency and propagation directions. In this work, we are interested in a signal with frequency, ω_3 , given by $\omega_3 = 2\omega_1 - \omega_2$, and propagation vector $\vec{k}_3 \approx 2\vec{k}_1 - \vec{k}_2$.

In order theoretically to study nd-FWM signal that emerge from a molecular system the Optical Bloch Equation (OBE) are the most common mathematical method employed (15). It is important to mention some of the approximations used to obtain the OBE used for this work: i) we employ a solvent transparent to the radiation in the dipole field-matter interaction, ii) the Rotating Wave Approximation (13) is not taken into consideration, which allows us to study the signal response out of the resonance frequency, and iii) the relaxation phenomenon is introduced in a phenomenological way.

Considering a homogeneous broadening of the spectral line and a local treatment for a spatial description, we can write the intensity for nd-FWM to the frequency $\omega_3 = 2\omega_1 - \omega_2$ as: $I_{ND-FWM} = \alpha |P(\omega_3 ; \omega_1, \omega_2)|$, where $P(\omega_3 ; \omega_1, \omega_2)$ is the corresponding Fourier component of the polarization vector, $\vec{P}(t)$, that oscillate at $\omega_3 = 2\omega_1 - \omega_2$.

The Fourier component to second order in the pump beam and to first order in the probe beam of the Polarization is given by (16, 17):

$$\begin{aligned}
 P(\omega_3 ; \omega_1, \omega_2) = & \\
 & iN\rho_D^{(0)} E_1^2(\omega_1) E_2^*(\omega_2) \left\{ 2m_{gr,ex}^4 \left(\frac{1}{D_3^-} - \frac{1}{(D_3^+)^*} \right) \right. \\
 & \left[\frac{1}{\Gamma} + \left[\frac{1}{D_2^+} + \frac{1}{D_1^-} + \frac{1}{(D_2^-)^*} + \frac{1}{(D_1^+)^*} \right] + \frac{1}{\lambda} \left[\frac{1}{D_1^-} + \frac{1}{(D_1^+)^*} \right] \right] + \\
 & \Delta m_{gr,ex}^2 m_{gr,ex}^2 \left[\left(\frac{1}{D_3^-} - \frac{1}{\beta} \right) \left[\frac{1}{D_\Delta^- D_2^+} + \frac{1}{D_1^- D_\Delta} + \frac{1}{D_1^- D_5^-} \right] - \right. \\
 & \left. \left(\frac{1}{(D_3^+)^*} - \frac{1}{\beta} \right) \left[\frac{1}{(D_\Delta^+)^* (D_2^-)^*} + \frac{1}{(D_1^+)^* (D_D^+)^*} + \frac{1}{(D_1^+)^* (D_5^+)^*} \right] \right] \left. \right\} \quad [11]
 \end{aligned}$$

In Equation [11], N represents the concentration of the push-pull molecules and ρ_D^0 is the population difference between Ψ_{ex} and Ψ_{gr} states at the equilibrium situation and for the zero field case; $E_1(\omega_1)$ and $E_2(\omega_2)$ are the amplitudes of the applied electric fields, $m_{gr,ex}$ is the transition dipole moment in Equation [9] and $\Delta m_{gr,ex} = m_{ex,ex} - m_{gr,gr}$.

The others quantities are defined by:

$$\Gamma = \frac{i}{T_1 - i\Delta}, \quad \beta = \frac{1}{T_1 - i\omega_3}, \quad \lambda = \frac{1}{T_1 - 2i\omega_1},$$

$$D_n^\pm = \frac{1}{T_2} + i(\omega_0 \pm \omega_n) \quad (\text{with } n = 1, 2, 3),$$

$$D_5^\pm = \frac{1}{T} + i(\omega_0 \pm 2\omega_1),$$

and finally

$$D_\omega^\pm = \frac{1}{T_2} + i(\omega_0 \pm \Delta)$$

where $\omega_0 = \frac{1}{\hbar} \sqrt{(V_0 + k\delta q_{eq.})^2 + 4t^2}$ is the Bohr frequency for push-pull molecules and $\Delta = \omega_1 - \omega_2$.

For simplicity reasons, we have expressed the Macroscopic Polarization as:

$$P(\omega_3 ; \omega_1, \omega_2) = Y(\omega_1, \omega_2) \xi(\omega_3 ; \omega_1, \omega_2), \quad [12]$$

where:

$$Y(\omega_1, \omega_2) = N\rho_D^{(0)} E_1^2(\omega_1) E_2^*(\omega_2) \quad [13]$$

and

$$\begin{aligned} \xi(\omega_3 ; \omega_1, \omega_2) = & i \left\{ 2m_{gr,ex}^4 \left(\frac{1}{D_3^-} - \frac{1}{(D_3^+)^*} \right) \right. \\ & \left[\frac{1}{\Gamma} + \left[\frac{1}{D_2^+} + \frac{1}{D_1^-} + \frac{1}{(D_2^-)^*} + \frac{1}{(D_1^+)^*} \right] + \frac{1}{\lambda} \left[\frac{1}{D_1^-} + \frac{1}{(D_1^+)^*} \right] + \right. \\ & \Delta m_{gr,ex}^2 m_{gr,ex}^2 \left[\left(\frac{1}{D_3^-} - \frac{1}{\beta} \right) \left[\frac{1}{D_{\Delta}^- D_2^+} + \frac{1}{D_1^- D_{\Delta}^+} + \frac{1}{D_1^- D_5^+} \right] - \right. \\ & \left. \left. \left(\frac{1}{(D_3^+)^*} - \frac{1}{\beta} \right) \left[\frac{1}{(D_{\Delta}^+)^* (D_2^-)^*} + \frac{1}{(D_1^+)^* (D_5^+)^*} + \frac{1}{(D_1^+)^* (D_5^+)^*} \right] \right] \left. \right\} \quad [14] \end{aligned}$$

4. Results

It can be seen from Equation [5] that $q_{eq.}$ and $f(q_{eq.})$ are linearly related to each other. However, Equation [6] leads to a non-linear equation in $q_{eq.}$ that can be solved iteratively. Thus, given V_0 and the initial value for $q_{eq.}$ the self-consistent determination of the coordinate $q_{eq.}$ involves the following steps: (i) evaluate the function $f(q_{eq.})$ according to Equation [6], (ii) calculate a value of $q_{eq.}$ by means of Equation [5], and (iii) repeat set (i) and (ii) until convergence is achieved. From this iterative approach, given V_0 we can calculate $q_{eq.}$, $f(q_{eq.})$, and $|P(\omega_3 ; \omega_1, \omega_2)|^2$.

For convenience, we have calculated $|\xi(\omega_3 ; \omega_1, \omega_2)|^2$, considering the factor $Y(\omega_1, \omega_2)$ as a constant value, keeping with fixed values the parameters involved in this term.

Calculations have been carried out using the following molecular parameters: $k = 33.55 \text{ eV/\AA}^2$, $t = 11 \text{ eV}$, $\delta q = -0.24 \text{ \AA}$, and $\mu_{CT} = 32D$, which are useful to treat molecules with electron donor and acceptor end groups connected by a hexatriene chain (11).

The results of the calculation of the nd-FWM spectrum can be presented as three-dimensional surfaces in the Figure 2, where the intensity for nd-FWM is illustrated as a function of the pump and probe

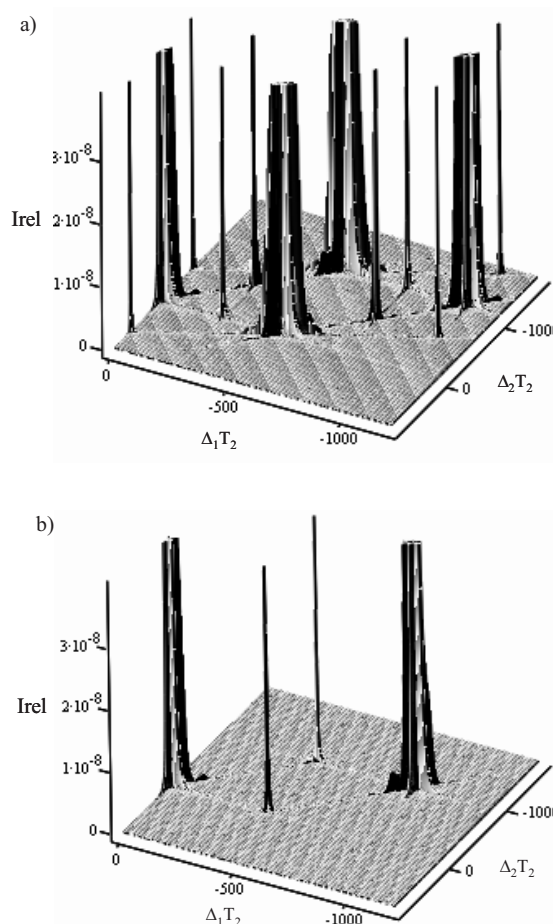


Figure 2. nd-FWM spectra vs. the pump and probe detunings $\Delta_1 T_2$ and $\Delta_2 T_2$, respectively, for the cases: a) $V_0 = \pm 1$ and b) $V_0 = 0$.

detuning, $(\omega_1 - \omega_0)T_2$ and $(\omega_2 - \omega_0)T_2$, respectively, for intervals $-\omega_0 \leq \omega_1 \leq \omega_0$ and $-2\omega_0 \leq \omega_2 \leq 2\omega_0$, and selected values of V_0 and T_1 / T_2 ratio.

In the case of general push-pull molecules, i.e. $V_0 \neq 0$, the nd-FWM spectrum contains twelve peaks (see Figure 2a) that are symmetric in intensity and position with the change in the resonance frequency from ω_i to $-\omega_i$ with $i = 1$ or 2 (Table 1). The peaks are numbered from 1 to 12, respectively, where the last six peaks are images of the first ones (Table 1). Moreover, the cases $\pm V_0$ generate identical results for the nd-FWM spectrum. In contrast, for $V_0 = 0$, i.e. cyanine molecules, only four peaks are observed in the Figure 2b: the peak 2, peak 6, and their respective images. This last result can be explained because for $V_0 = 0 \rightarrow \Delta m_{gr.ex} = 0$, therefore the second term in Equation [11] vanishes and as consequence the nd-FWM signal is simplified.

In Figures 3-5 we have illustrated the results of the $|\xi(\omega_3; \omega_1, \omega_2)|^2$ calculations as a function of the fraction of CT state of the electronic ground state (f) to the follows cases

of the ratio T_1 / T_2 : a) $T_1 = 0.1T_2$, b) $T_1 = T_2$, and c) $T_1 = 10T_2$. Moreover, we have taken into account the frequency coordinate of the maximal intensity for each peak (as it is presented in Table 1). These calculations were carried out for the first six peaks of the Table 1. These changes in the relaxation times can be associated with the employ of solvents of different dielectric constant (15).

In Figures 3-5 that increasing the ratio T_1 / T_2 from a) to c), increase the intensity of the peaks 1, 2 (Figure 3) and peak 4 (Figure 4). In these cases, the increase is of two orders of magnitude for each order of magnitude in the increasing of T_1 / T_2 . For the peaks 3 (Figure 4), 5 and 6 (Figure 5) the intensity remain unaffected. Moreover, the intensity of the peak 2 is non-zero at $f = 0.5$, contrasting with the others peaks. This fact can be explained because each peak is governed by some terms of polarization expression, which define its behavior. Considering this aspect, it is possible to observe that the relative polarization expressions of the peaks 1, 2 and 4 have an direct dependence with the longitudinal relaxation times, fact that is not true for the case of the peaks 3, 5

Table 1
Frequencies ω_1 , ω_2 and ω_3 for the twelve peaks in the nd-FWM spectrum

	Pump Frequency (cm ⁻¹)	Probe Frequency (cm ⁻¹)
Peak 1	ω_0	$2 \omega_0$
Peak 2	ω_0	ω_0
Peak 3	ω_0	0
Peak 4	$\omega_0 / 2$	ω_0
Peak 5	$\omega_0 / 2$	0
Peak 6	0	ω_0
Peak 7	$-\omega_0$	$-2 \omega_0$
Peak 8	$-\omega_0$	$-\omega_0$
Peak 9	$-\omega_0$	0
Peak 10	$-\omega_0 / 2$	$-\omega_0$
Peak 11	$-\omega_0 / 2$	0
Peak 12	0	$-\omega_0$

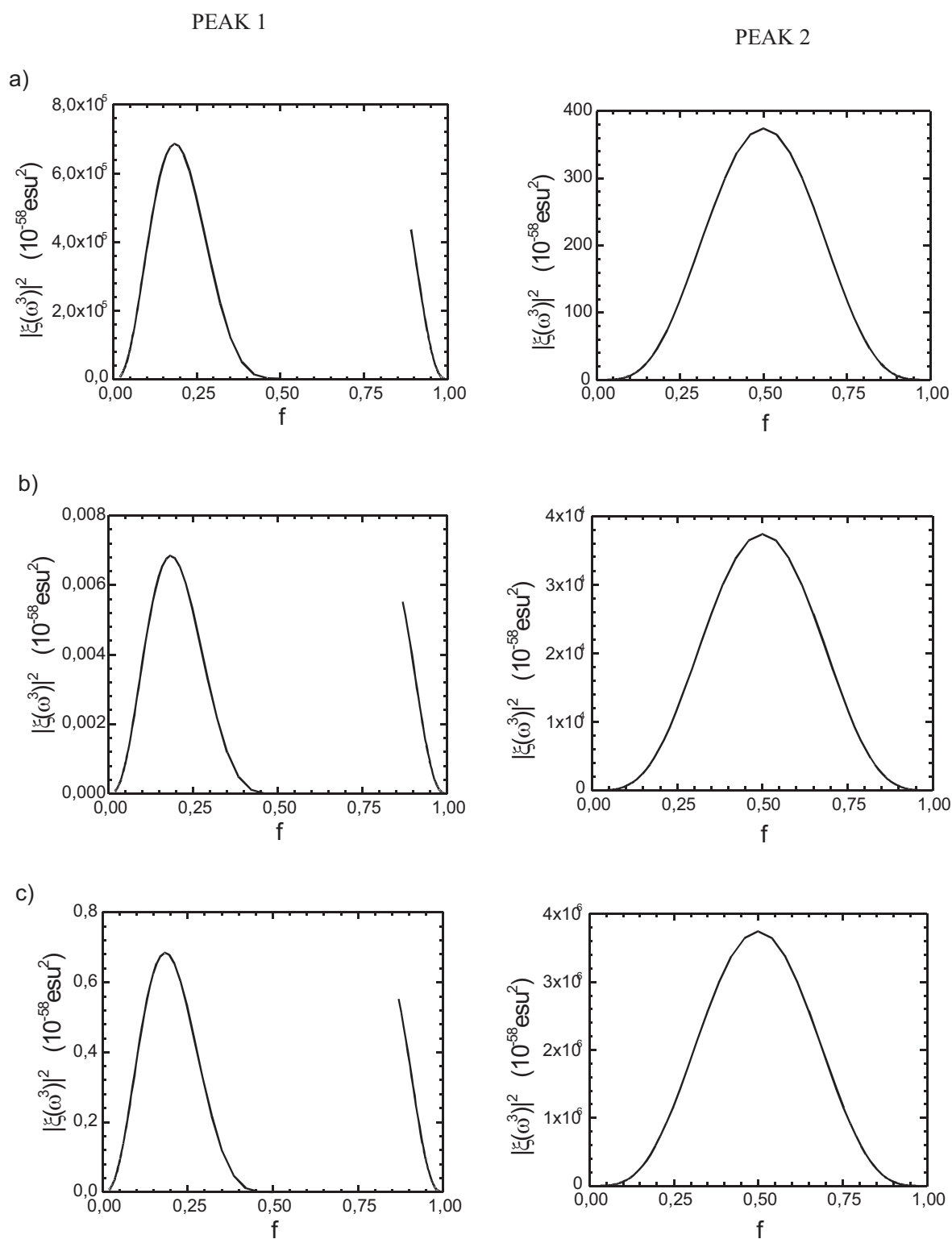


Figure 3. Factor $|\xi(\omega_3 ; \omega_1, \omega_2)|^2$ vs. f for the peaks 1 and 2 when a) $T_1 = 0.1T_2$, b) $T_1 = T_2$, and c) $T_1 = 10T_2$.

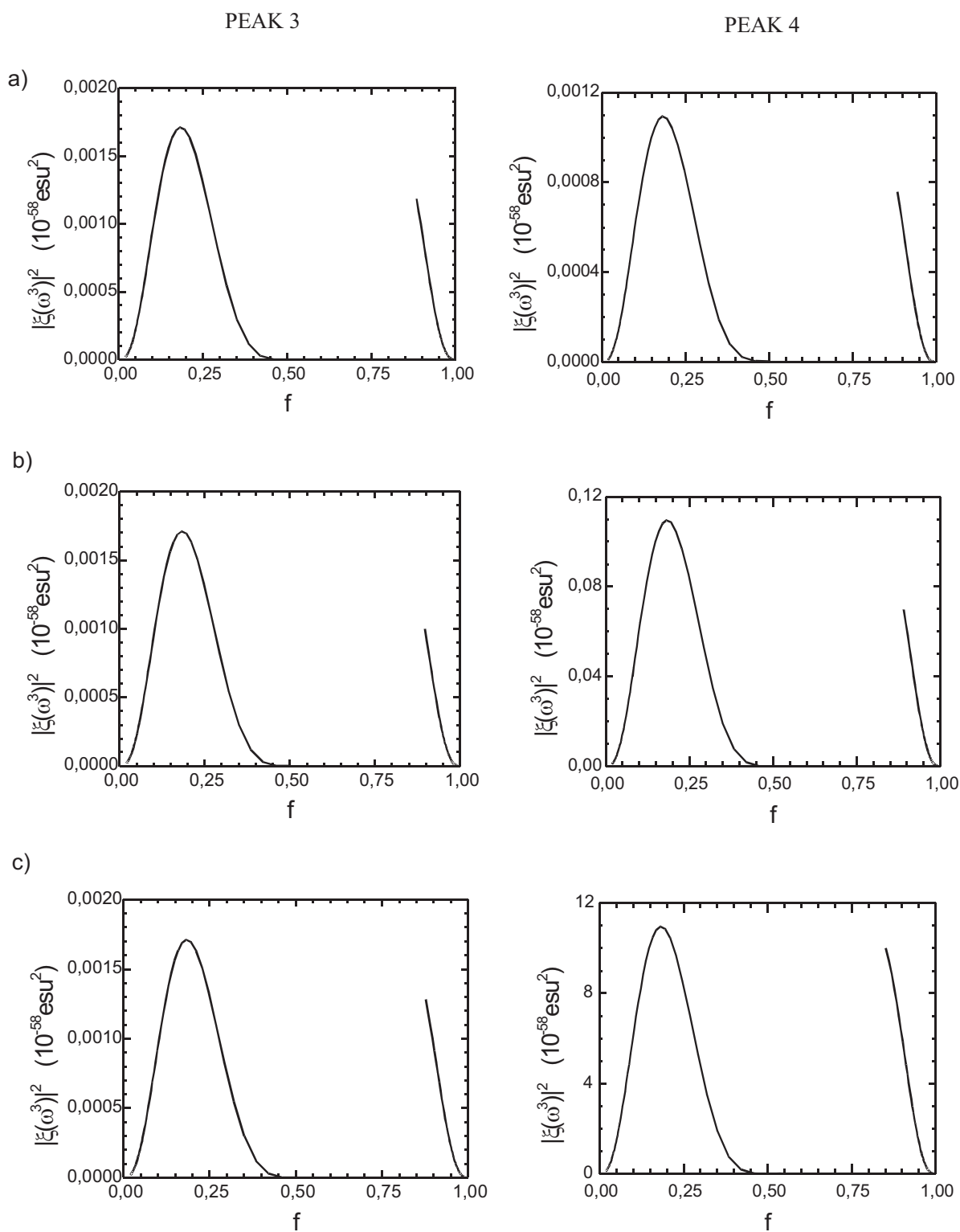


Figure 4. Factor $|\xi(\omega_3; \omega_1, \omega_2)|^2$ vs. f for the peaks 3 and 4 when a) $T_1 = 0.1T_2$, b) $T_1 = T_2$, and c) $T_1 = 10T_2$.

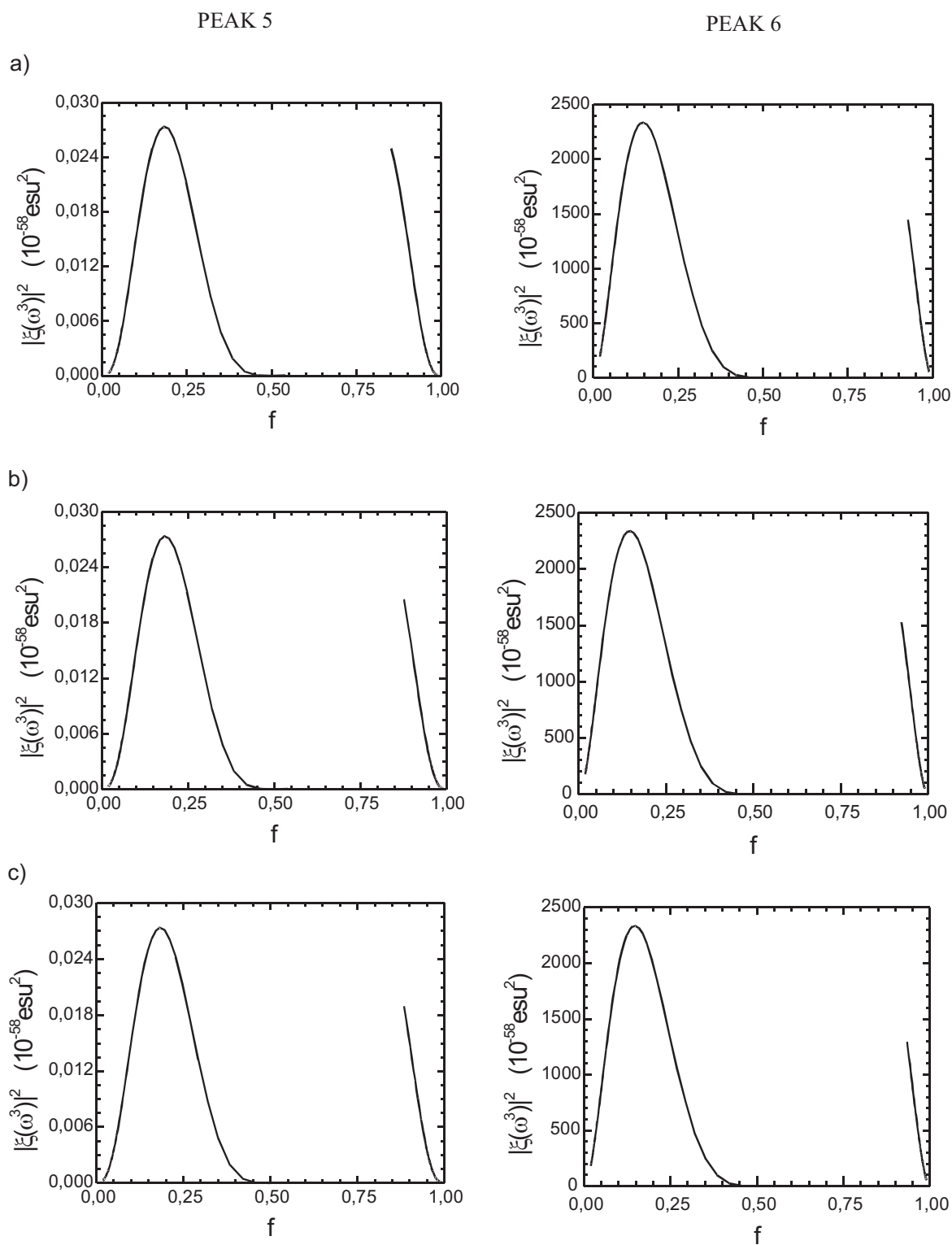


Figure 5. Factor $|\xi(\omega_3 ; \omega_1, \omega_2)|^2$ vs. f for the peaks 5 and 6 when a) $T_1 = 0.1T_2$, b) $T_1 = T_2$, and c) $T_1 = 10T_2$.

Table 2
The maximum value of the factor $|\xi(\omega_3; \omega_1, \omega_2)|^2$ as function of the ratio T_1 / T_2 for the peaks 1-6

	$T_1 = 0.1T_2$	$T_1 = T_2$	$T_1 = 10T_2$	f_{opt}
Peak 1	6.853×10^{-5}	6.844×10^{-3}	0.6844	0.818 0.182
Peak 2	373.986	37392.917	3739289.984	0.5
Peak 3	1.712×10^{-3}	1.711×10^{-3}	1.711×10^{-3}	0.818 0.182
Peak 4	1.094×10^{-3}	0.1095	10.950	0.818 0.182
Peak 5	2.738×10^{-2}	2.738×10^{-2}	2.738×10^{-2}	0.818 0.182
Peak 6	2336.610	2336.677	2336.797	0.852 0.148

and 6, which are only proportional to the transversal relaxations times.

In the Table 2 we presented the maximum value of $|\xi(\omega_3; \omega_1, \omega_2)|^2$ as function of the ratio T_1 / T_2 for each one of the peaks 1-6. A general observation from this table shows that when $T_1 = 0.1T_2$, the larger intensity corresponds to the peak 6 for $f = 0.148$ (i.e. $V_0 = 1668$ eV and $q_{\text{eq.}} = -0.084$ Å) and $f = 0.852$ (i.e. $V_0 = -1668$ eV and $q_{\text{eq.}} = 0.084$ Å). For $T_1 = T_2$ and $T_1 = 10T_2$, the higher intensity is associated to the peak 2 when $f = 0.5$, i.e. for the cyanine molecule.

5. Concluding Remarks

We have presented the nd-FWM spectrum for cyanines ($V_0 = 0$) and D-A polyenes ($V_0 \neq 0$). In first place, we have obtained nd-FWM signal spectra in the frequency space for the cases of $V_0 = \pm 1$ and $V_0 = 0$, observing differences between them. For $V_0 = \pm 1$ a spectrum with twelve peaks is obtained, 6 of them with symmetry in position and intensity respect to another six. In the second case, only four peaks are present, due to that $\Delta m_{\text{ex-gr}} = 0$, which induces only the re-

sponse of specific resonant terms in the polarization expression. The last one corresponds to the specific case of cyanine molecules. In the other hand, the behavior of the factor $|\xi(\omega_3; \omega_1, \omega_2)|^2$ (directly proportional to the macroscopic polarization) has been studied as a function of the parameter f , considering the different changes in the ratio between the relaxation times T_1 / T_2 . We have observed for the peaks 1, 2 and 4, an increasing in two orders of magnitude in this quantity with the increasing in an order of magnitude in T_1 / T_2 . This fact is due to the direct proportionality of response of these peaks with the longitudinal relaxation time, while the peaks do not experiment this changes, because of the absence of the dependence mentioned before.

Acknowledgments

The present work was supported by the Fondo Nacional de Ciencia, Tecnología e Innovación (FONACIT) (grants S1-2001000672 and G-97000593) and by the Decanato de Investigaciones de la Universidad Simón Bolívar (grant GID-13).

Bibliographic References

1. CHEMLA D.S., ZYSS J. (Ed.). **Nonlinear Optical Properties of Organic Molecules and Crystals**, Academic Press, New York (USA), 1987.
2. PRASAD P.N., WILLIAMS D.J. **Introduction to Nonlinear Optical Effects in Molecules and Polymers**, Wiley, New York (USA), 1990.
3. KANIS D.R., RATNER M.A., MARKS T.J. **Chem Rev** 94: 195, 1994.
4. Special edition: **Adv Chem Phys** 85, 1993.
5. CHENG L.T., TAM W., STEVENSON S.H., MEREDITH G.R., RIKKEN G., MARDER S.R. **J Phys Chem** 95: 10631, 1991.
6. RISSER S.M., BERATAN D.N., MARDER S.R. **J Am Chem Soc** 115: 7719, 1993.
7. NIE W. **Adv Mater** 5: 520, 1993.
8. CAMMI R., MENNICCI B., TOMASI J. **J Am Chem Soc** 120: 8834, 1998.
9. MARDER S.R., PERRY J.W., BOURHILL G., GORMAN C.B., TIEMANN B.G., MANSUR K. **Science**, 261: 186, 1993.
10. LU D., CHEN G., PERRY J.W., GODDARD III W.A. **J Am Chem Soc** 116: 10679, 1994.
11. BLOCH D., DUCLOY M. **J Opt Soc Am** 73: 635, 1983.
12. LEVENSON M.D. **Introduction to nonlinear spectroscopy**, Academic Press, New York (USA), 1982.
13. MUKAMEL S. **Principles of Nonlinear Optical Spectroscopy**, Oxford, New York (USA), 1995.
14. BLOCH D., DUCLOY M. **J Opt Soc Am** 73: 635, 1983.
15. PAZ J.L., CUSATI T., SALAZAR M.C., HERNÁNDEZ A.J. **J Mol Spect** 211: 198, 2002.
16. CUSATI T., PAZ J.L., SQUITIERI E., SALAZAR M.C., HERNÁNDEZ A.J., MUJICA V. **Mol Phys** 100: 1587, 2002.